Journal of Applied Mechanics and Technical Physics, Vol. 49, No. 2, pp. 239–252, 2008

STABILITY OF WAVY DOWNFLOW OF FILMS CALCULATED BY THE NAVIER–STOKES EQUATIONS

Yu. Ya. Trifonov

UDC 532.51

The process of downflow of viscous films on a smooth surface is analyzed theoretically with the use of the full Navier–Stokes equations. The limits of applicability of the asymptotic and integral approaches to the description of waves on falling films are determined. Various nonlinear wavy downflow regimes are calculated in a wide range of the Reynolds and Kapitsa numbers, and stability of these regimes is studied. For low values of the Kapitsa number, the results of the asymptotic approach are demonstrated to be inapplicable almost for all Reynolds numbers. For high values of the Kapitsa number, the solution obtained by the asymptotic method starts to differ significantly from the result obtained by solving the Navier–Stokes equations beginning from moderate Reynolds numbers. For high Reynolds numbers, the wavelength of neutral disturbances is independent of the flow rate of the liquid, and the phase velocity of neutral disturbances is close to the velocity of the free surface. Calculations of nonlinear wavy regimes with moderate Reynolds numbers predict the existence of internal vortex zones. It is shown that there are only a few families of steady traveling solutions (a countable set of different families of such solutions was obtained in calculations by the integral model).

Key words: *viscous film flow, waves, stability.*

1. INTRODUCTION AND FORMULATION OF THE PROBLEM

The study of film flows was started by Nusselt [1] who obtained an exact solution of the Navier–Stokes equations for a free downflow of a thin layer of a viscous liquid on a smooth wall and by Kapitsa [2] who performed experiments to consider the main wavy regimes of film flows and proposed an integral approach to theoretical investigations of this phenomenon. The linear stability of a waveless film downflow to free surface perturbations was considered in [3, 4]. It was shown that a vertical film flow contains unstable disturbances for all Reynolds numbers. Subsequent extensive theoretical research involved an analysis of nonlinear waves of falling films. Investigations were performed either with the use of a nonlinear evolution equation for the film thickness (see, e.g., [5–11]) derived from the asymptotic expansion of the original Navier–Stokes equations or within the framework of the integral approach (see, e.g., [9–14]). It was found that there exists a countable set of different one-parameter families of steady traveling solutions branching off from each other (for each particular family, the parameter is the wavelength or the wavenumber of the nonlinear solution). An analysis of linear stability of different solutions allowed us to identify two families of waves. It is only for these families that there exists an interval of wavelengths where nonlinear solutions are stable. There are only a few theoretical papers where the wavy film flow is considered with the use of the Navier–Stokes equations. Chin et al. [15] solved the Orr–Sommerfeld equations numerically and obtained data on the linear stability of waveless downflow for high Reynolds numbers ($\mathrm{Re} > 100$). Salamon et al. [16] and Bach and Villadsen [17] performed Navier–Stokes calculations to obtain the evolution of various initial perturbations on

Kutateladze Institute of Thermophysics, Siberian Division, Russian Academy of Sciences, Novosibirsk 630090; trifonov@itp.nsc.ru. Translated from Prikladnaya Mekhanika i Tekhnicheskaya Fizika, Vol. 49, No. 2, pp. 98–112, March–April, 2008. Original article submitted January 9, 2007.

the surface of falling films. The studies were performed for moderate Reynolds numbers. The main objective of the present work was the study of various wavy regimes of film downflow with the use of the full Navier–Stokes equations.

2. GOVERNING EQUATIONS

2.1. System of Nonlinear Equations. Film downflow on an inclined plane is described by a system of the Navier–Stokes equations in rectangular coordinates with appropriate boundary conditions:

$$\frac{\partial u}{\partial t}+u\,\frac{\partial u}{\partial x}+v\,\frac{\partial u}{\partial y}=-\frac{\partial P}{\partial x}+\frac{1}{\varepsilon\,\mathrm{Re}}\Big(3+\frac{\partial^2 u}{\partial y^2}+\varepsilon^2\,\frac{\partial^2 u}{\partial x^2}\Big),$$

$$\varepsilon^2\Big(\frac{\partial v}{\partial t}+u\,\frac{\partial v}{\partial x}+v\,\frac{\partial v}{\partial y}\Big)=-\frac{\partial P}{\partial y}-\frac{3\tan\theta}{\mathrm{Re}}+\frac{\varepsilon}{\mathrm{Re}}\Big(\frac{\partial^2 v}{\partial y^2}+\varepsilon^2\,\frac{\partial^2 v}{\partial x^2}\Big),$$

$$\frac{\partial u}{\partial x}+\frac{\partial v}{\partial y}=0,$$

$$u=v=0,\qquad y=0,$$

$$\frac{\partial u}{\partial y}+\varepsilon^2\,\frac{\partial v}{\partial x}+4\varepsilon^2\,\frac{\partial v}{\partial y}\,\frac{\partial H}{\partial x}\,\frac{1}{1-\varepsilon^2(\partial H/\partial x)^2}=0,\qquad y=H(x,t),$$

$$P=P_a+\frac{2\varepsilon}{\mathrm{Re}}\,\frac{\partial v}{\partial y}\,\frac{1+\varepsilon^2(\partial H/\partial x)^2}{1-\varepsilon^2(\partial H/\partial x)^2}-\frac{(3\,\mathrm{Fi})^{1/3}\varepsilon^2}{\mathrm{Re}^{5/3}}\,\frac{\partial^2 H/\partial x^2}{[1+\varepsilon^2(\partial H/\partial x)^2]^{3/2}},\qquad y=H(x,t),$$

$$v=\frac{\partial H}{\partial t}+u\,\frac{\partial H}{\partial x},\qquad y=H(x,t).$$

Here $H(x,t)$ is the local film thickness, u and v are the components of the velocity vector in the x and y directions, respectively, P is the pressure in the liquid, P_a is the atmospheric pressure, t is the time, and θ is the slope of the x axis counted from the vertical direction. The equations are written in dimensionless form. The dimensionless quantities are related to the appropriate dimensional quantities (indicated by the asterisk):

$$x=\frac{x^*}{L},\quad y=\frac{y^*}{H_0},\quad t=\frac{u_0t^*}{L},\quad u=\frac{u^*}{u_0},\quad v=\frac{v^*}{\varepsilon u_0},\quad P=\frac{P^*}{\rho u_0^2},\quad H=\frac{H^*}{H_0},$$

$$\mathrm{Re}=\frac{u_0H_0}{\nu}=\frac{g\cos\theta H_0^3}{3\nu^2},\quad \varepsilon=\frac{H_0}{L},\quad \mathrm{Fi}=\frac{(\sigma/\rho)^3}{g\cos\theta\nu^4}.$$

Here ν is the kinematic viscosity, ρ is the density of the liquid, σ is the surface tension, L is the wave period, Re is the Reynolds number, and Fi is the film number.

Using the transformation of coordinates $t_1=t$, $x_1=x-ct$, $\eta=y/H(x-ct,t)$ (c is the phase velocity; the flow domain in the new variables is known: $\eta\in[0,1]$), we obtain the global coordinate system in the following form (the subscript 1 at the new variables of time and coordinate is omitted):

$$\frac{\partial u}{\partial t}-c\,\frac{\partial u}{\partial x}+\eta_t\,\frac{\partial u}{\partial\eta}=-\frac{\partial P}{\partial x}-\eta_x\,\frac{\partial P}{\partial\eta}$$

$$+\frac{1}{\varepsilon\,\mathrm{Re}}\Big[3+\eta_y^2\,\frac{\partial^2 u}{\partial\eta^2}+\varepsilon^2\Big(\frac{\partial^2 u}{\partial x^2}+\eta_x^2\,\frac{\partial^2 u}{\partial\eta^2}+2\eta_x\,\frac{\partial^2 u}{\partial x\,\partial\eta}+(\eta_{x\xi}+\eta_x\eta_{x\eta})\frac{\partial u}{\partial\eta}\Big)\Big]-\eta_y\,\frac{\partial uv}{\partial\eta}-\frac{\partial u^2}{\partial x}-\eta_x\,\frac{\partial u^2}{\partial\eta};\quad(2.1)$$

$$\eta_y\,\frac{\partial P}{\partial\eta}=-\frac{3\tan\theta}{\mathrm{Re}}+\frac{\varepsilon}{\mathrm{Re}}\Big[\eta_y^2\,\frac{\partial^2 v}{\partial\eta^2}+\varepsilon^2\Big(\frac{\partial^2 v}{\partial x^2}+\eta_x^2\,\frac{\partial^2 v}{\partial\eta^2}+2\eta_x\,\frac{\partial^2 v}{\partial x\,\partial\eta}+(\eta_{x\xi}+\eta_x\eta_{x\eta})\,\frac{\partial v}{\partial\eta}\Big)\Big]$$

$$-\varepsilon^2\Big(\frac{\partial v}{\partial t}-c\,\frac{\partial v}{\partial x}+\eta_t\,\frac{\partial v}{\partial\eta}+\frac{\partial uv}{\partial x}+\eta_x\,\frac{\partial uv}{\partial\eta}+\eta_y\,\frac{\partial v^2}{\partial\eta}\Big);\quad(2.2)$$

$$v(t,x,\eta) = -H(t,x)u(t,x,\eta)\eta_x - \frac{\partial}{\partial x}\Big(H\int\limits_0^\eta u(t,x,\eta')\,d\eta'\Big); \tag{2.3}$$

$$\frac{\partial H}{\partial t} + \frac{\partial}{\partial x}\Big(H(t,x)\int\limits_0^1 (u(t,x,\eta') - c)\,d\eta'\Big) = 0; \tag{2.4}$$

$$u(t,x,\eta) = 0, \qquad \eta = 0; \tag{2.5}$$

$$P - P_a = \frac{2\varepsilon}{\mathrm{Re}}\,\eta_y\,\frac{\partial v}{\partial \eta}\,\frac{1+\varepsilon^2(\partial H/\partial x)^2}{1-\varepsilon^2(\partial H/\partial x)^2} - \varepsilon^2\,\mathrm{We}\,\frac{\partial^2 H/\partial x^2}{[1+\varepsilon^2(\partial H/\partial x)^2]^{3/2}}, \qquad \eta = 1; \tag{2.6}$$

$$\Big(\frac{\partial u}{\partial \eta} + \varepsilon^2 H\,\frac{\partial v}{\partial x} - \varepsilon^2\,\frac{\partial H}{\partial x}\,\frac{\partial v}{\partial \eta}\Big)\Big[1 - \varepsilon^2\Big(\frac{\partial H}{\partial x}\Big)^2\Big] + 4\varepsilon^2\,\frac{\partial v}{\partial \eta}\,\frac{\partial H}{\partial x} = 0, \qquad \eta = 1. \tag{2.7}$$

Here $\mathrm{We} = (3\,\mathrm{Fi})^{1/3}/\,\mathrm{Re}^{5/3}$ is the Weber number, $\eta_x = -(\eta\,\partial H/\partial x)/H$, $\eta_y = 1/H$, $\eta_t = -\eta(\partial H/\partial t - c\,\partial H/\partial x)/H$, $\eta_{x\eta} = -(\partial H/\partial x)/H$, and $\eta_{x\xi} = -(\eta_x/H)\,\partial H/\partial x - (\eta\partial^2 H/\partial x^2)/H$. Below we find the steady-state solutions of system (2.1)–(2.7) [$H_b(x)$, $u_b(x,\eta)$, $v_b(x,\eta)$, and $P_b(x,\eta)$] and study their linear stability. One of the solutions (the trivial one) can be easily written:

$$\begin{gathered} H_b^0(x) = 1, \qquad u_b^0(x,\eta) = 1.5(2\eta - \eta^2), \\ v_b^0(x,\eta) = 0, \qquad P_b^0(x,\eta) = P_a + 3\tan\theta(1-\eta)/\,\mathrm{Re}\,. \end{gathered} \tag{2.8}$$

Other steady-state solutions can be constructed only numerically. It follows from Eqs. (2.1)–(2.7) that the flow is determined by three independent quantities: θ, Fi, and Re. The spatial wave period L is an internal parameter. In constructing the steady-state solutions numerically, we used the spectral method [18] developed for analyzing the film flow on a corrugated surface:

$$u_b(x,\eta) = \frac{1}{2}\,U_1(x) + \sum_{m=2}^{M} U_m(x)T_{m-1}(\eta_1), \qquad \eta_1 = 2\eta - 1,$$

$$U_m(x) = U_m^0 + \sum_{\substack{n=-N/2+1 \\ n\neq 0}}^{N/2-1} U_m^n \exp(2\pi i n x), \qquad (U_m^{-n})^* = U_m^n, \quad m = 1,\ldots,M.$$

Here $T_m(\eta_1)$ are the Chebyshev polynomials; the asterisk indicates complex conjugation.

It should be noted that, in contrast to the algorithm developed in [18], the harmonics U_m^n in the case considered are supplemented by the harmonics in the expansion of the film thickness $H_b(x)$. For given $M(N-1)$ values of the real and imaginary parts of the harmonics U_m^n and $N-1$ values of the harmonics H^n, the velocity $v_b(x,\eta)$ is uniquely determined by Eq. (2.3), and the pressure $P_b(x,\eta)$ is found from Eqs. (2.2) and (2.6). The numerical algorithm starts from the initial approximation of the harmonics U_m^n and H^n [for example, from the trivial solution of Eq. (2.8) in the neighborhood of the neutral curve], which is then refined by the Newton method with the use of Eq. (2.1) in the space (n,m) and Eq. (2.4):

$$H_b(x) = (1 - c\langle H_b(x)\rangle) \Big/ \int\limits_0^1 (u_b(x,\eta') - c)\,d\eta'.$$

Here $\langle\,\cdot\,\rangle$ is the mean over the wavelength. The phase velocity c is determined from the condition of symmetry with respect to the shift of the origin of the x coordinate. In the expansion of the film thickness, we can assume that the phase of one harmonic is known and consider the velocity c as an unknown instead of this phase. The Jacobi matrix is calculated by a finite-difference scheme. The basis functions do not satisfy the boundary conditions (2.5) and (2.7) automatically. As a consequence, we obtain $(M+3)(N-1)$ nonlinear algebraic equations for determining $(M+1)(N-1)$ unknowns, i.e., the system is overdetermined. In the present work, we reject $2(N-1)$

equations corresponding to two last (small) Chebyshev polynomials in the expansion of Eq. (2.1); instead of them, we use the boundary conditions (2.5) and (2.7). In tuning the calculation procedure, we checked other possible methods of reducing the number of equations. The result almost coincide in all cases if the function $u(x,\eta)$ is approximated with sufficient accuracy. The values of N and M were varied in calculations to satisfy the conditions $|U_m^{N/2-1}|/\sup|U_m^n| < 10^{-3}$ for all m and $|U_M^n|/\sup|U_m^n| < 10^{-3}$ for all n. Small differences in the solutions for different N and M (in the case of satisfactory approximation of the velocity field) additionally confirms that the calculation procedure is correct.

2.2. Stability of Steady-State Solutions. Substituting the expressions

$$H = H_b(x) + \hat{H}(x)\exp(-\gamma t) + \text{c.c.}, \qquad u = u_b(x,\eta) + \hat{u}(x,\eta)\exp(-\gamma t) + \text{c.c},$$

$$v = v_b(x,\eta) + \hat{v}(x,\eta)\exp(-\gamma t) + \text{c.c}, \qquad P = P_b(x,\eta) + \hat{P}(x,\eta)\exp(-\gamma t) + \text{c.c},$$

$$\eta_x = \bar{\eta}_x + \hat{\eta}_x, \qquad \eta_y = \bar{\eta}_y + \hat{\eta}_y, \qquad \eta_t = \bar{\eta}_t + \hat{\eta}_t, \qquad \eta_{x\eta} = \bar{\eta}_{x\eta} + \hat{\eta}_{x\eta}, \qquad \eta_{x\xi} = \bar{\eta}_{x\xi} + \hat{\eta}_{x\xi},$$

$$\hat{\eta}_x = -\bar{\eta}_x\frac{\hat{H}}{H_b} - \frac{\eta}{H_b}\frac{d\hat{H}}{dx}, \qquad \hat{\eta}_y = -\bar{\eta}_y\frac{\hat{H}}{H_b}, \qquad \hat{\eta}_t = -\bar{\eta}_t\frac{\hat{H}}{H_b} - \frac{\eta}{H_b}\Big(-\gamma\hat{H} - c\frac{d\hat{H}}{dx}\Big),$$

$$\hat{\eta}_{x\eta} = -\bar{\eta}_{x\eta}\frac{\hat{H}}{H_b} - \frac{1}{H_b}\frac{d\hat{H}}{dx}, \qquad \hat{\eta}_{x\xi} = -\bar{\eta}_{x\xi}\frac{\hat{H}}{H_b} - \frac{1}{H_b}\Big(\hat{\eta}_x\frac{dH_b}{dx} + \bar{\eta}_x\frac{d\hat{H}}{dx} + \eta\frac{d^2\hat{H}}{dx^2}\Big)$$

(complex-conjugate quantities with respect to the disturbance are denoted by c.c.); the quantities marked by the bar are obtained with the substitution of the steady-state solution) into Eqs. (2.1)–(2.7) and linearizing these equations, we obtain a system of equations in eigenvalues with periodic (or constant if stability of the trivial solution is studied) coefficients along the x coordinate:

$$a_1^1(x)\hat{H} + a_2^1(x)\frac{d\hat{H}}{dx} + a_3^1(x)\int_0^1 \hat{u}\,d\eta' + a_4^1(x)\frac{d}{dx}\int_0^1 \hat{u}\,d\eta' = \gamma\hat{H}; \tag{2.9}$$

$$a_1^2(x,\eta)\hat{H} + a_2^2(x,\eta)\frac{d\hat{H}}{dx} + a_3^2(x,\eta)\frac{d^2\hat{H}}{dx^2} + a_4^2(x,\eta)\hat{u} + a_5^2(x,\eta)\frac{\partial\hat{u}}{\partial x} + a_6^2(x,\eta)\frac{\partial\hat{u}}{\partial\eta}$$

$$+ a_7^2\frac{\partial^2\hat{u}}{\partial x^2} + a_8^2(x,\eta)\frac{\partial^2\hat{u}}{\partial\eta^2} + a_9^2(x,\eta)\frac{\partial^2\hat{u}}{\partial x\,\partial\eta} + a_{10}^2(x,\eta)\hat{v} + a_{11}^2(x,\eta)\frac{\partial\hat{v}}{\partial\eta}$$

$$+ \frac{\partial\hat{P}}{\partial x} + a_{12}^2(x,\eta)\frac{\partial\hat{P}}{\partial\eta} = \gamma\Big[b_1^2(x,\eta)\hat{H} + \hat{u}\Big]; \tag{2.10}$$

$$\hat{u} = 0, \qquad \eta = 0; \tag{2.11}$$

$$a_1^4(x)\hat{H} + a_2^4(x)\frac{d\hat{H}}{dx} + a_3^4(x)\frac{\partial\hat{u}}{\partial\eta} + a_4^4(x)\frac{\partial\hat{v}}{\partial x} + a_5^4(x)\frac{\partial\hat{v}}{\partial\eta} = 0, \qquad \eta = 1; \tag{2.12}$$

$$a_1^5(x,\eta)\hat{H} + a_2^5(x,\eta)\frac{d\hat{H}}{dx} + a_3^5(x,\eta)\hat{u} + a_4^5(x)\int_0^\eta \hat{u}\,d\eta' + a_5^5(x)\frac{\partial}{\partial x}\int_0^\eta \hat{u}\,d\eta' + \hat{v} = 0; \tag{2.13}$$

$$a_1^6(x,\eta)\hat{H} + a_2^6(x,\eta)\frac{d\hat{H}}{dx} + a_3^6(x,\eta)\frac{d^2\hat{H}}{dx^2} + \int_\eta^1 \Big(a_4^6(x,\eta')\hat{u} + a_5^6(x,\eta')\frac{\partial\hat{u}}{\partial x} + a_6^6(x,\eta')\frac{\partial\hat{u}}{\partial\eta'}$$

$$+ a_7^6(x,\eta')\hat{v} + a_8^6(x,\eta')\frac{\partial\hat{v}}{\partial x} + a_9^6(x,\eta')\frac{\partial\hat{v}}{\partial\eta'} + a_{10}^6\frac{\partial^2\hat{v}}{\partial x^2} + a_{11}^6(x,\eta')\frac{\partial^2\hat{v}}{\partial\eta'^2} + a_{12}^6(x,\eta')\frac{\partial^2\hat{v}}{\partial x\,\partial\eta'}\Big)d\eta'$$

$$+\frac{1}{H_b(x)}\,\hat{P}(x,\eta)\Big|_{\eta=1}-\frac{\hat{P}(x,\eta)}{H_b(x)}=\gamma\Big(b_1^6(x,\eta)\hat{H}+\varepsilon^2\int\limits_{\eta}^{1}\hat{v}\,d\eta'\Big);\tag{2.14}$$

$$\hat{P}(x,\eta)\Big|_{\eta=1}=a_1^7(x)\hat{H}+a_2^7(x)\,\frac{d\hat{H}}{dx}+a_3^7(x)\,\frac{d^2\hat{H}}{dx^2}+a_4^7(x)\,\frac{\partial\hat{v}}{\partial\eta}\Big|_{\eta=1}.$$

The coefficients a_j^i and b_j^i in Eqs. (2.9)–(2.14) are real functions and are expressed via the solution of the steady-state problem as

$$a_1^1=\frac{d}{dx}\int\limits_0^1(u_b-c)\,d\eta',\qquad a_2^1=\int\limits_0^1(u_b-c)\,d\eta',\qquad a_3^1=\frac{dH_b}{dx},\qquad a_4^1=H_b,$$

$$a_1^2=-\frac{\bar\eta_t}{H_b}\,\frac{\partial u_b}{\partial\eta}-\frac{\bar\eta_x}{H_b}\,\frac{\partial P_b}{\partial\eta}+\frac{1}{\varepsilon\,\mathrm{Re}}\Big\{2\,\frac{\bar\eta_y^2}{H_b}\,\frac{\partial^2u_b}{\partial\eta^2}+\varepsilon^2\Big[2\,\frac{\bar\eta_x^2}{H_b}\,\frac{\partial^2u_b}{\partial\eta^2}+2\,\frac{\bar\eta_x}{H_b}\,\frac{\partial^2u_b}{\partial x\,\partial\eta}$$
$$+\Big(\frac{\bar\eta_{x\xi}}{H_b}+3\,\frac{\bar\eta_x\bar\eta_{x\eta}}{H_b}\Big)\frac{\partial u_b}{\partial\eta}\Big]\Big\}-\frac{\bar\eta_y}{H_b}\,\frac{\partial\,(u_bv_b)}{\partial\eta}-\frac{\bar\eta_x}{H_b}\,\frac{\partial u_b^2}{\partial\eta},$$

$$a_2^2=-\frac{\eta}{H_b}\,\frac{\partial P_b}{\partial\eta}+\frac{\varepsilon}{\mathrm{Re}}\Big[2\,\frac{\bar\eta_x\eta}{H_b}\,\frac{\partial^2u_b}{\partial\eta^2}+2\,\frac{\eta}{H_b}\,\frac{\partial^2u_b}{\partial x\,\partial\eta}+2\Big(\frac{\bar\eta_{x\eta}\eta}{H_b}+\frac{\bar\eta_x}{H_b}\Big)\frac{\partial u_b}{\partial\eta}\Big]-\frac{\eta}{H_b}\,(2u_b-c)\,\frac{\partial u_b}{\partial\eta},$$

$$a_3^2=\frac{\varepsilon}{\mathrm{Re}}\,\frac{\eta}{H_b}\,\frac{\partial u_b}{\partial\eta},\qquad a_4^2=\bar\eta_y\,\frac{\partial v_b}{\partial\eta}+2\,\frac{\partial u_b}{\partial x}+2\bar\eta_x\,\frac{\partial u_b}{\partial\eta},\qquad a_5^2=2u_b,$$

$$a_6^2=\bar\eta_t-\frac{\varepsilon}{\mathrm{Re}}\,(\bar\eta_{x\xi}+\bar\eta_x\bar\eta_{x\eta})+\bar\eta_yv_b+2\bar\eta_xu_b,\qquad a_7^2=-\frac{\varepsilon}{\mathrm{Re}},$$

$$a_8^2=-\frac{\varepsilon\eta_x^2}{\mathrm{Re}}-\frac{\eta_y^2}{\varepsilon\,\mathrm{Re}},\qquad a_9^2=-\frac{2\varepsilon\bar\eta_x}{\mathrm{Re}},$$

$$a_{10}^2=\bar\eta_y\,\frac{\partial u_b}{\partial\eta},\qquad a_{11}^2=\bar\eta_yu_b,\qquad a_{12}^2=\bar\eta_x,\qquad b_1^2=-\frac{\eta}{H_b}\,\frac{\partial u_b}{\partial\eta},$$

$$a_1^4=(1-K^2)\varepsilon^2\,\frac{\partial v_b}{\partial x}\Big|_{\eta=1},\qquad K=\varepsilon\,\frac{dH_b}{dx},$$

$$a_2^4=\Big[-(1-K^2)\varepsilon^2\,\frac{\partial v_b}{\partial\eta}-2\varepsilon K\Big(\frac{\partial u_b}{\partial\eta}+\varepsilon^2H_b\,\frac{\partial v_b}{\partial x}-\varepsilon K\,\frac{\partial v_b}{\partial\eta}\Big)+4\varepsilon^2\,\frac{\partial v_b}{\partial\eta}\Big]\Big|_{\eta=1},$$

$$a_3^4=1-K^2,\qquad a_4^4=(1-K^2)\varepsilon^2H_b,\qquad a_5^4=-\varepsilon K(1-K^2)+4\varepsilon K,$$

$$a_1^5=\frac{\partial}{\partial x}\int\limits_0^\eta u_b\,d\eta',\qquad a_2^5=\int\limits_0^\eta u_b\,d\eta'-u_b\eta,\qquad a_3^5=\bar\eta_xH_b,\qquad a_4^5=\frac{dH_b}{dx},\qquad a_5^5=H_b,$$

$$a_1^6=\int\limits_\eta^1\Bigg(-\frac{\varepsilon^2\bar\eta_t}{H_b}\,\frac{\partial v_b}{\partial\eta'}-\frac{\bar\eta_y}{H_b}\,\frac{\partial P_b}{\partial\eta'}+\frac{\varepsilon}{\mathrm{Re}}\Big\{2\,\frac{\bar\eta_y^2}{H_b}\,\frac{\partial^2v_b}{\partial\eta'^2}+\varepsilon^2\Big[2\,\frac{\bar\eta_x^2}{H_b}\,\frac{\partial^2v_b}{\partial\eta'^2}$$
$$+2\,\frac{\bar\eta_x}{H_b}\,\frac{\partial^2v_b}{\partial x\,\partial\eta'}+\Big(\frac{\bar\eta_{x\xi}}{H_b}+3\,\frac{\bar\eta_x\bar\eta_{x\eta}}{H_b}\Big)\frac{\partial v_b}{\partial\eta'}\Big]\Big\}-\frac{\varepsilon^2\bar\eta_y}{H_b}\,\frac{\partial v_b^2}{\partial\eta'}-\frac{\varepsilon^2\bar\eta_x}{H_b}\,\frac{\partial(u_bv_b)}{\partial\eta'}\Bigg)d\eta',$$

$$a_2^6=\frac{\varepsilon^3}{\mathrm{Re}\,H_b}\int\limits_\eta^1\Big(2\bar\eta_x\eta'\,\frac{\partial^2v_b}{\partial\eta'^2}+2\eta'\,\frac{\partial^2v_b}{\partial x\,\partial\eta'}+2(\bar\eta_{x\eta}\eta'+\bar\eta_x)\,\frac{\partial v_b}{\partial\eta'}\Big)d\eta'-\frac{\varepsilon^2}{H_b}\int\limits_\eta^1\Big(\eta'\,\frac{\partial\,((u_b-c)v_b)}{\partial\eta'}\Big)\,d\eta',$$

$$a_3^6 = \frac{\varepsilon^3}{\mathrm{Re}}\,\frac{1}{H_b}\int\limits_{\eta}^{1}\eta'\,\frac{\partial v_b}{\partial \eta'}\,d\eta', \qquad a_4^6 = \varepsilon^2\Big(\frac{\partial v_b}{\partial x} + \bar\eta_x\,\frac{\partial v_b}{\partial \eta}\Big), \qquad a_5^6 = \varepsilon^2 v_b, \qquad a_6^6 = \varepsilon^2\bar\eta_x v_b,$$

$$a_7^6 = \varepsilon^2\Big(2\bar\eta_y\,\frac{\partial v_b}{\partial \eta} + \frac{\partial u_b}{\partial x} + \bar\eta_x\,\frac{\partial u_b}{\partial \eta}\Big), \qquad a_8^6 = \varepsilon^2(u_b - c),$$

$$a_9^6 = \varepsilon^2\bar\eta_t - \frac{\varepsilon^3}{\mathrm{Re}}\,(\bar\eta_{x\xi} + \bar\eta_x\bar\eta_{x\eta}) + \varepsilon^2(2\bar\eta_y v_b + \bar\eta_x u_b), \qquad a_{10}^6 = -\frac{\varepsilon^3}{\mathrm{Re}},$$

$$a_{11}^6 = -\frac{\varepsilon}{\mathrm{Re}}\,\bar\eta_y^2 - \frac{\varepsilon^3}{\mathrm{Re}}\,\bar\eta_x^2, \qquad a_{12}^6 = -\frac{2\varepsilon^3}{\mathrm{Re}}\,\bar\eta_x, \qquad b_1^6 = -\frac{\varepsilon^2}{H_b}\int\limits_{\eta}^{1}\Big(\eta'\,\frac{\partial v_b}{\partial \eta}\Big)\,d\eta',$$

$$a_1^7 = -\frac{2\varepsilon}{\mathrm{Re}}\,\frac{\bar\eta_y}{H_b}\,\frac{1+K^2}{1-K^2}\,\frac{\partial v_b}{\partial \eta}\Big|_{\eta=1},$$

$$a_2^7 = \frac{3\varepsilon^3 K\,\mathrm{We}}{(1+K^2)^{5/2}}\Big(\frac{d^2H_b}{dx^2} + \frac{1}{\varepsilon_1}\,\frac{d^2 f}{dx^2}\Big) + \frac{8\varepsilon^2 K}{\mathrm{Re}}\,\frac{\bar\eta_y}{(1-K^2)^2}\,\frac{\partial v_b}{\partial \eta}\Big|_{\eta=1},$$

$$a_3^7 = -\frac{\varepsilon^2\,\mathrm{We}}{(1+K^2)^{3/2}}, \qquad a_4^7 = \frac{2\varepsilon}{\mathrm{Re}}\,\bar\eta_y\,\frac{1+K^2}{1-K^2}.$$

It follows from the Floquet theorem that the solutions of system (2.9)–(2.14) bounded in terms of the x coordinate can be presented as

$$\begin{pmatrix}\hat H\\ \hat u\\ \hat v\\ \hat P\end{pmatrix} = \begin{pmatrix} \displaystyle\sum_{n=-N/2+1}^{n=N/2-1}\hat H_n\exp(2\pi i n x) \\ \displaystyle\frac{1}{2}\sum_{n=-N/2+1}^{n=N/2-1}\hat u_{1n}\exp(2\pi i n x) + \sum_{m=2}^{M}T_{m-1}(2\eta-1)\sum_{n=-N/2+1}^{n=N/2-1}\hat u_{mn}\exp(2\pi i n x) \\ \displaystyle\frac{1}{2}\sum_{n=-N/2+1}^{n=N/2-1}\hat v_{1n}\exp(2\pi i n x) + \sum_{m=2}^{M}T_{m-1}(2\eta-1)\sum_{n=-N/2+1}^{n=N/2-1}\hat v_{mn}\exp(2\pi i n x) \\ \displaystyle\frac{1}{2}\sum_{n=-N/2+1}^{n=N/2-1}\hat P_{1n}\exp(2\pi i n x) + \sum_{m=2}^{M}T_{m-1}(2\eta-1)\sum_{n=-N/2+1}^{n=N/2-1}\hat P_{mn}\exp(2\pi i n x) \end{pmatrix}\exp(2\pi i Q x).$$

Here the real parameter is $Q \in [0,1]$. After substitution of these expressions into Eqs. (2.9)–(2.14), the problem reduces to a generalized problem in eigenvalues for complex matrices of the general form:

$$A\hat x = \gamma B\hat x, \qquad \hat x = \begin{pmatrix}\hat H_n\\ \hat u_{mn}\\ \hat v_{mn}\\ \hat P_{mn}\end{pmatrix}. \tag{2.15}$$

The matrices A and B, which have the dimension $[(3M+1)(N-1),(3M+1)(N-1)]$, were constructed numerically. A succession of different unit vectors of disturbances was set, and the columns of the matrices A and B were calculated. As in calculating the nonlinear steady-state solutions, we rejected $2(N-1)$ equations corresponding to two last (small) Chebyshev polynomials in the expansion of Eq. (2.10) and used the boundary conditions (2.11), (2.12) instead of them.

To evaluate the stability of the solution $[H_b(x), u_b(x,\eta), v_b(x,\eta)$, and $P_b(x,\eta)]$, we have to analyze $(3M+1)(N-1)$ eigenvalues for each value of the parameter Q. The solution is stable is the real parts of all eigenvalues are greater than or equal to zero. Disturbances with the zero value of the parameter Q should be noted specially. Such disturbances have the same period as the initial solution. Instability to this class of disturbances means that such a regime cannot be realized in the experiment. Solutions unstable to disturbances with $Q \neq 0$ can be observed in experiments in certain segments of the flow, where the disturbances did not yet have enough time to develop or were artificially suppressed.

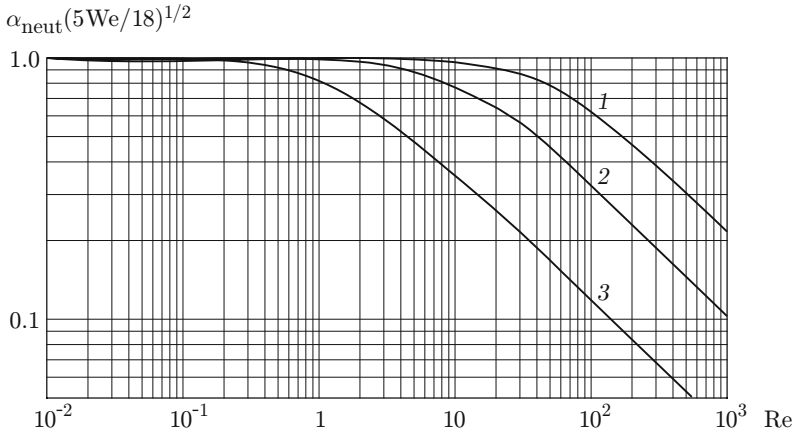

Fig. 1. Wavenumbers of neutral disturbances for a film flowing down a vertical wall, obtained by Navier–Stokes calculations for $\text{Fi}^{1/11} = 10$ (1), 5 (2), and 2 (3).

3. CALCULATION RESULTS

3.1. Stability of the Waveless Film Flowing Down a Smooth Wall. Benjamin [3] solved the Orr–Sommerfeld equation for a film flowing down an inclined plane with the use of expansion with respect to the small parameter. For $\text{Re} > (\text{Re}_{\text{cr}})_B$, all disturbances with wavelengths $\lambda^* > (\lambda^*_{\text{neut}})_B$ (the quantities indicated by the asterisk are dimensional) are unstable and increase with time (disturbances with $\lambda^* < (\lambda^*_{\text{neut}})_B$ decay with time). The following relations were obtained [3] for the critical Reynolds number $(\text{Re}_{\text{cr}})_B$ above which wave formation begins and for the wavelength of the neutral disturbance $(\lambda^*_{neut})_B$:

$$(\text{Re}_{\text{cr}})_B = \frac{5}{6}\,\tan\theta, \qquad \frac{2\pi H_0}{(\lambda^*_{\text{neut}})_B}\sqrt{\frac{5\,\text{We}}{18}} = \sqrt{1 - \frac{5\tan\theta}{6\,\text{Re}}}.$$

Figure 1 shows the results of calculating stability ($\alpha_{\text{neut}} \equiv 2\pi H_0/\lambda^*_{\text{neut}}$) of a waveless film flow by the linearized Navier–Stokes equations (2.9)–(2.14) in the case of a vertical wall ($\theta = 0$). The calculations were performed for three values of the film number Fi. The value $\text{Fi}^{1/11} = 10$ is close to the corresponding number for water or a cryogenic liquid (nitrogen at the saturation line at atmospheric pressure); the values $\text{Fi}^{1/11} = 5$ and 2 correspond to the aqueous solution of alcohol and glycerin (see, e.g., [10]). The results plotted in Fig. 1 can be readily compared with the calculations by the asymptotic theory [3] [$(\alpha_{\text{neut}})_B\sqrt{5\,\text{We}/18} = 1$ for all values of Re and Fi]. Stability calculations were also performed for slopes of the flow plane $\theta = 45$ and 80°. The critical Reynolds numbers Re_{cr} corresponding to the beginning of wave formation coincide with those calculated by the asymptotic theory [3]. For $\text{Re} < \text{Re}_{\text{cr}}$, all disturbances decay, and the real parts of all eigenvalues of problem (2.15) are greater than zero (in the entire range of the values of the parameter Q). For $\text{Re} > \text{Re}_{\text{cr}}$ (at least, up to $\text{Re} = 1000$) and for $Q < Q_{\text{neut}}$, the spectrum of eigenvalues always has the only unstable mode whose wavelength is L/Q. For $Q > Q_{\text{neut}}$, the real parts of all eigenvalues of problem (2.15) are greater than zero, and the disturbances decay with time.

Note, the number of the Chebyshev polynomials M in disturbance approximations performed was varied within a wide range (from 10 to 50). The dependences of the neutral disturbance wavelength on the Reynolds number plotted in Fig. 1 were obtained for $M = 25$ (in the entire range of variation of Re) and remain unchanged with a further increase in M. For high Reynolds numbers, the dependences in Fig. 1 have an asymptotic curve for each value of Fi (which is a straight line in logarithmic coordinates).

The results obtained allows us to draw the following conclusions.

In the neighborhood of the critical number of wave formation, the results on stability of the waveless flow calculated by the linearized Navier–Stokes equations agree with the results obtained by the asymptotic theory [3]. The region where these results are consistent becomes substantially smaller with decreasing film number. In the case of a film flowing down a vertical wall, the wavelength of the neutral disturbance in this region decreases with increasing Reynolds number: $\lambda^*_{\text{neut}} \sim \sqrt{\sigma/(\rho g\,\text{Re})}$, and shorter and shorter disturbances become unstable. The phase velocity of the neutral disturbance in this region is close to the doubled velocity on the film surface.

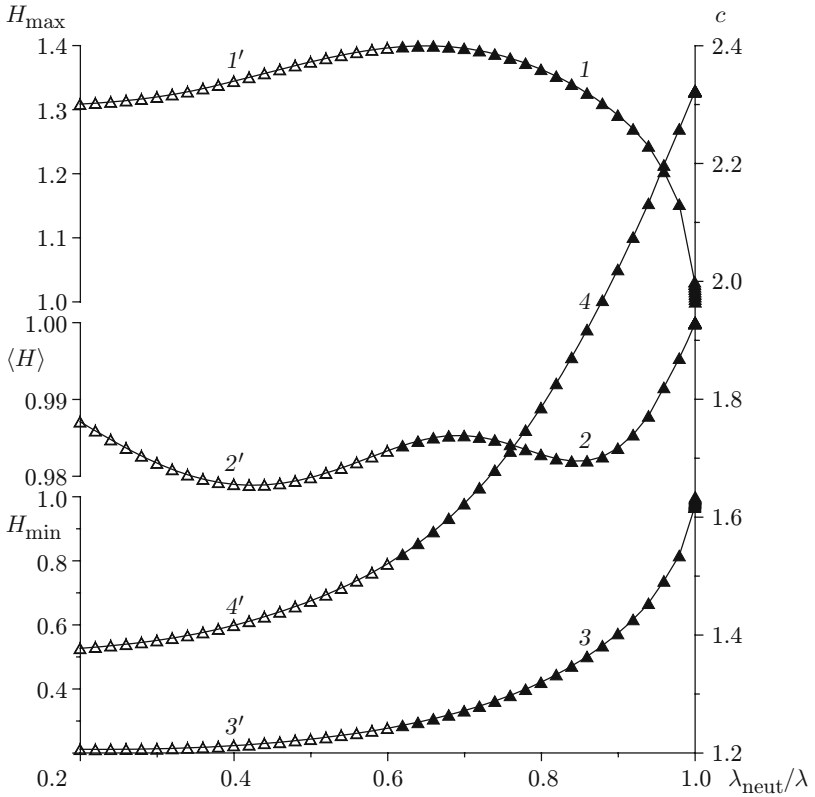

Fig. 2. Basic wave characteristics of nonlinear solutions of the first family and regions of stability of these solutions, obtained by the Navier–Stokes calculations for Ka = 10 and Re = 100: the curves show the solutions stable (1–4) and unstable (1′–4′) with respect to disturbances with the period λ equal to the period of the nonlinear solution; curves 1–3 and 1′–3′ show the maximum film thickness $H_{\max}$ (1 and 1′), the mean film thickness $\langle H \rangle$ (2 and 2′), and the minimum film thickness $H_{\min}$ (3 and 3′); curves 4 and 4′ show the phase velocity c.

For high Reynolds numbers, the dependences obtained imply that the wavelength of the neutral disturbance is determined only by the physical properties of the liquid and by the slope of the plane of the film flow [$\lambda^*_{\text{neut}} = C\sqrt{\sigma/(\rho g)}$, where $C = C(\theta, \text{Fi}^{1/11})$] and does not depend on the flow rate of the liquid. The phase velocity of the neutral disturbances is close to the velocity of the free surface.

3.2. Nonlinear Wavy Regimes Branching Off from the Trivial Solution and Their Stability for a Film Flowing Down a Smooth Vertical Surface. Steady traveling wavy solutions of system (2.1)–(2.7) (called the first family of waves in what follows) branch off from the line of the loss of stability of the trivial solution. In considering these solutions, we confine ourselves to the case of a vertical wall. The problem has two external parameters: the Kapitsa number $\text{Ka} = \text{Fi}^{1/11}$ and $\text{Re}\,/\,\text{Ka}$. The wavelength (or the wavenumber) is one of the internal characteristics of the solution for a family of nonlinear waves. In what follows, the wavelength is usually normalized to the wavelength of the neutral disturbance for the corresponding values of Ka and Re.

Figure 2 shows the results calculated for nonlinear waves and their stability for Ka = 10 and $\text{Re}\,/\,\text{Ka} = 10$. Similar calculations were performed for $\text{Re}\,/\,\text{Ka} = 1.0$ and 0.1. In all cases, branching occurs in the "soft" regime, and the solutions continue to the region of linear instability of the trivial solution up to the small values of the wavenumber $\alpha/\alpha_{\text{neut}} = 0.2$. The mean film thickness is close to unity in the entire range of parameters, and the wave amplitude is extremely small for $\text{Re}\,/\,\text{Ka} = 0.1$. For Ka = 10, the long waves of the first family are unstable to disturbances with a period equal to the period of the nonlinear solution [disturbances with $Q = 0$ in problem (2.9)–(2.14)]. When the stability of the solution to disturbances with $Q = 0$ is studied, the spectrum of eigenvalues consists of one zero value (consequence of translational symmetry), several real eigenvalues, and a large number of pairs of complex-conjugate roots. As the wavenumber changes, the spectrum of eigenvalues also changes; new

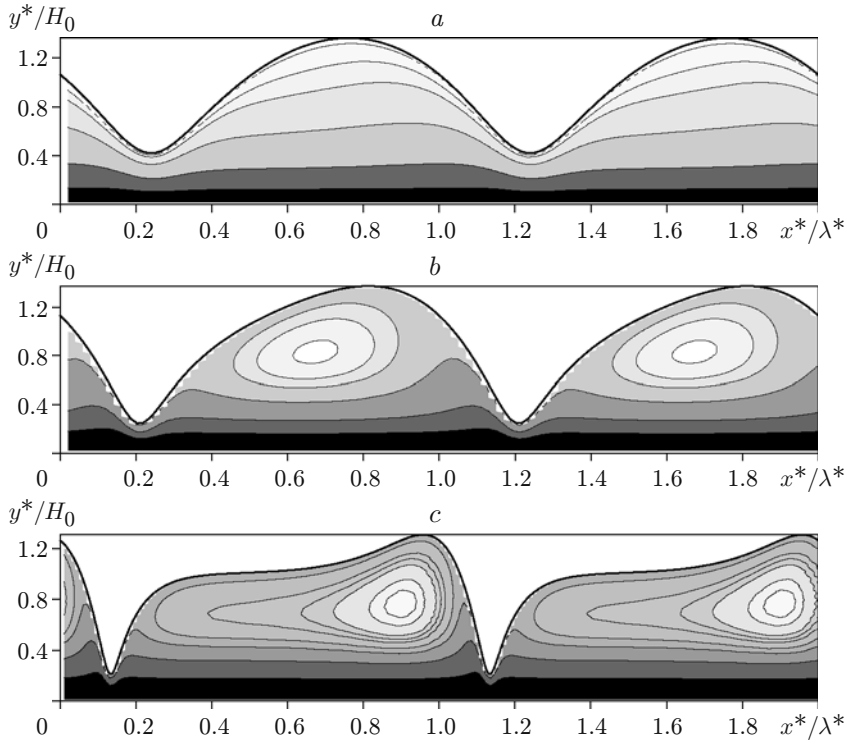

Fig. 3. Profile of the film thickness for the solutions of the first family and isolines of the stream function in a coordinate system moving with the phase velocity of the wave for Ka = 10 and Re = 100: $\lambda_{\text{neut}}/\lambda = 0.8$ (a), 0.5 (b), and 0.2 (c).

complex-conjugate pairs of roots may appear, or a complex-conjugate pair may transform to two real roots. In the case of the loss of stability of the waves of the first family (see Fig. 2), the dependence of the real part of the complex-conjugate pair of eigenvalues on $\lambda_{\text{neut}}/\lambda$ passes through the zero point. Figure 3 shows the typical profiles of the solutions of this family for Re = 100 and Ka = 10 and also the isolines of the stream function $\Psi(x, \eta)$ in a coordinate system moving with the phase velocity of the wave:

$$\Psi(x, \eta) = \int_0^\eta (u - c)H \, d\eta'.$$

The presence of a vortex in the structure of the stream function for this value of the Reynolds number should be noted.

Figure 4 shows the calculated results for nonlinear waves and their stability for Ka = 2 and Re / Ka = 1. Similar calculations were performed for Re / Ka = 10.0 and 0.1. In this case, branching also occurs in the "soft" regime, and the solutions continue to the region of linear instability of the trivial solution. Figure 5 shows the typical wave profiles for Re = 20 and Ka = 2 and also the isolines of the stream function $\Psi(x, \eta)$ in a coordinate system moving with the phase velocity of the wave. A large number of Fourier harmonics has to be used in calculating long waves for Ka = 2. Stability of solutions with respect to disturbances with $Q = 0$ was studied only up to comparatively small ratios $\lambda_{\text{neut}}/\lambda \approx 0.4$. For Ka = 2, no unstable solutions were found (except for the case with Re = 0.2). It should be noted that there is a qualitative difference in the profiles of the long waves of the first family for Ka = 10 and Ka = 2: these are successions of solitary dips in the first case and solitary humps with a steep leading front in the second case. For Re / Ka = 10 and Ka = 2, in addition, there appears a vortex inside the wave hump with decreasing wavenumber (see Fig. 5), and a further decrease in the wavenumber requires an extremely large number of the Fourier harmonics. Calculation of long solitary dips with a vortex for Ka = 10 involves no significant difficulties.

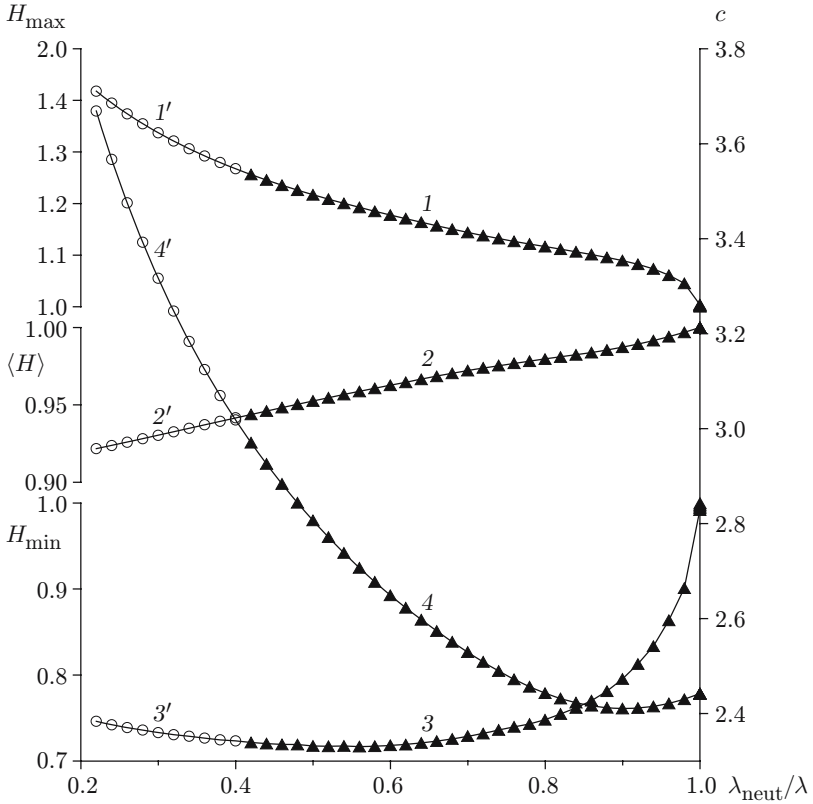

Fig. 4. Basic wave characteristics of nonlinear solutions of the first family and regions of stability of these solutions, obtained by the Navier–Stokes calculations for Ka = 2 and Re = 2: curves 1–4 show the solutions stable with respect to disturbances with the period λ equal to the period of the nonlinear solution; curves 1′–4′ show the regions where the solution was not studied; curves 1–3 and 1′–3′ show the maximum film thickness $H_{\max}$ (1 and 1′), the mean film thickness $\langle H \rangle$ (2 and 2′), and the minimum film thickness $H_{\min}$ (3 and 3′); curves 4 and 4′ show the phase velocity c.

Figure 6 shows the wave characteristics calculated for an increased parameter Re / Ka. The calculations were started from the solutions of the first family obtained for Re / Ka = 0.1. The experiments [2] made it possible to formulate the criterion of the beginning of wave formation on the surface of falling films Re / Ka > 0.61. It follows from the data in Fig. 6 that the maximum rate of variation of the main wave characteristics is reached in the vicinity of the value Re / Ka = 0.61. For high values of Re / Ka, the maximum and minimum dimensionless thicknesses of the film tend to a constant value.

Thus, for one set of parameters (e.g., $\lambda_{neut}/\lambda = 0.4$, Re / Ka = 1, and Ka = 10), the solutions can be obtained by different methods: 1) by changing the wavenumber with Re / Ka = const; 2) by changing the parameter Re / Ka with a fixed value of $\lambda_{\text{neut}}/\lambda$. A question of solution uniqueness arises. This issue was considered in [6, 9] with the use of a simple evolution equation (valid for low Reynolds numbers) and in [13, 14] within the framework of the integral model. In both cases, there exist special lines $\lambda(Q)$ where the solution of the first family with the wavelength λ loses its stability with respect to disturbances with this value of Q. Among these special lines, there are lines where the real eigenvalue changes its sign for all values $Q \in [0; 0.5]$. New families of steady traveling periodic solutions branch off along these lines for rational values of Q. Thus, these models have a countable set of different families of steady traveling solutions. Such degeneration is not observed in considering nonlinear waves with the use of the Navier–Stokes equations. For finite values of $Q \neq 1/2$, no lines were found with simultaneous vanishing of the real and imaginary parts of some eigenvalue. For $Q = 1/2$, the spectrum of eigenvalues of problem (2.9)–(2.14) consists of real and complex-conjugate pairs of numbers. In this case, when the real eigenvalue passes through the zero point, a new family of steady traveling solutions branches off (and the period is doubled) (Fig. 7).

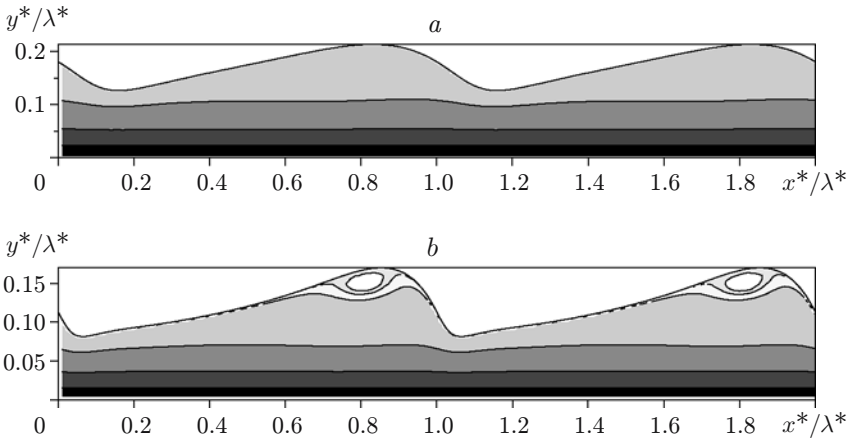

Fig. 5. Profile of the film thickness for solutions of the first family and isolines of the stream function in a coordinate system moving with the phase velocity of the wave for Ka = 2 and Re = 20: $\lambda_{\text{neut}}/\lambda = 0.78$ (a) and 0.56 (b).

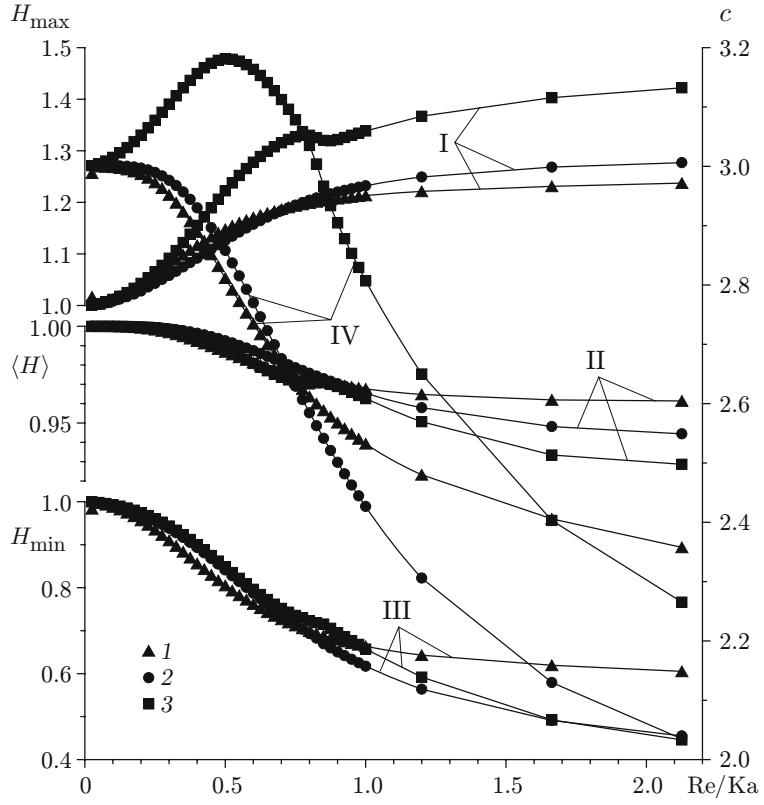

Fig. 6. Basic wave characteristics of nonlinear solutions calculated by the Navier–Stokes equations for Ka = 10: curves I–III show the maximum film thickness $H_{\max}$ (I), the mean film thickness $\langle H \rangle$ (II), and the minimum film thickness $H_{\min}$ (III); curve IV shows the phase velocity c; $\lambda_{\text{neut}}/\lambda = 0.8$ (1), 0.6 (2), and 0.4 (3).

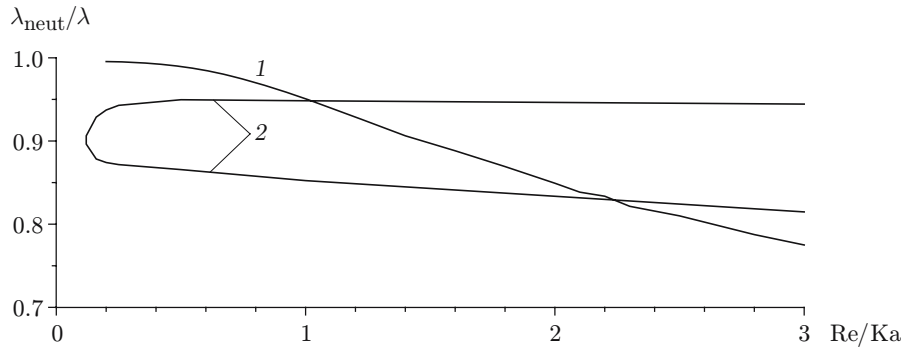

Fig. 7. Lines along which new steady traveling regimes with a doubled period branch off from solutions of the first family: Ka = 10 (1) and 2 (2).

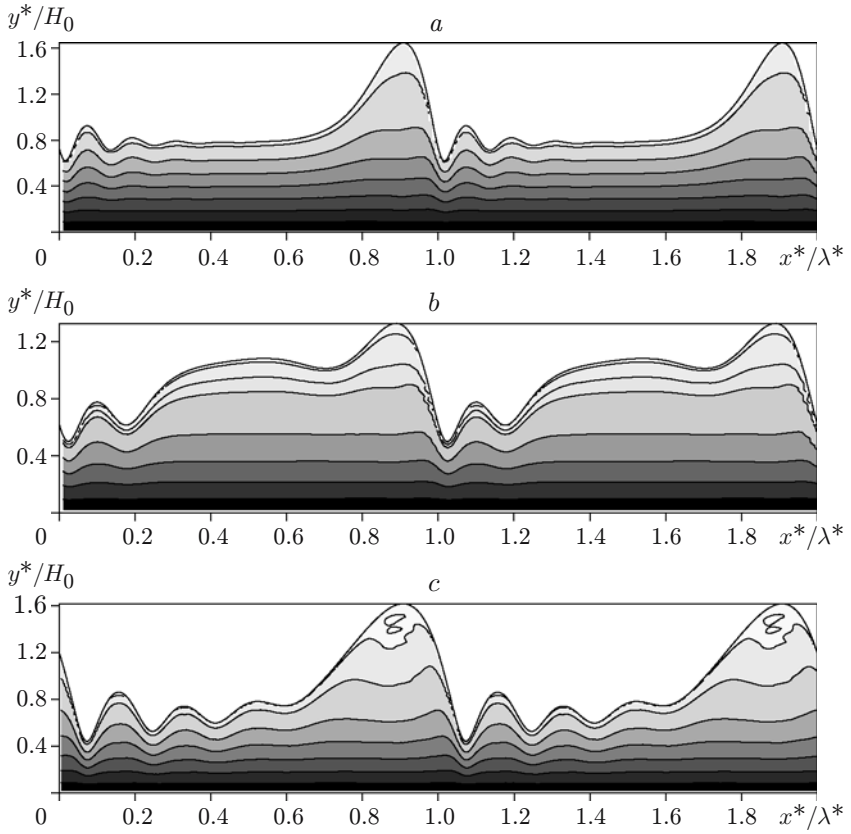

Fig. 8. Profile of the film thickness and isolines of the stream function for Ka = 10: (a) $\lambda_{\text{neut}}/\lambda = 0.22$ and Re = 10; (b) $\lambda_{\text{neut}}/\lambda = 0.2$ and Re = 20 (b); (c) $\lambda_{\text{neut}}/\lambda = 0.26$ and Re = 24.1.

Figure 8a shows the profile of the solution for the second family of nonlinear waves branched off from curve 1 in Fig. 7 for Re / Ka = 1. In contrast to the long wave of the first family, (solitary dip in Fig. 3), here we have a solitary hump; in addition, there are "ripples" on the leading front. For wavenumbers greater than the value corresponding to Re / Ka = 2 on curve 1 (see Fig. 7), there arise waves of another type (see Fig. 8b), which cannot be obtained by continuation of solitary humps or solitary dips with the parameter Re / Ka being varied (see Fig. 8c). Thus, for Ka = 10, the Navier–Stokes equations predict the existence of different types of long waves and, correspondingly, different families of solutions. These families in the plane of parameters (Re / Ka, $\lambda_{\text{neut}}/\lambda$) are interrelated in a complicated manner. For instance, for Re / Ka = 1, solitary humps can be obtained either by

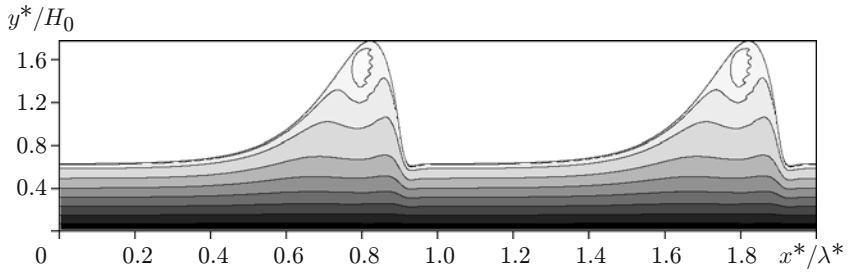

Fig. 9. Profile of the film thickness and isolines of the stream function in a coordinate system moving with the phase velocity of the wave for Ka = 2, $\lambda_{\text{neut}}/\lambda = 0.32$, and Re = 4.6 [the solution is continued from the wave of the first family with increasing Re (beginning from Re = 0.2) and $\lambda_{\text{neut}}/\lambda = \text{const}$].

branching from curve 1 in Fig. 7 and continuation by the parameter $\lambda_{\text{neut}}/\lambda$, or by branching from the waves of the first family calculated with increasing Re / Ka (beginning from Re / Ka = 0.1) and for $\lambda_{\text{neut}}/\lambda = \text{const}$.

The situation for Ka = 2 is simpler. Different types of long waves were not found in calculations. New solutions branched off with doubling of the period on the upper part of curve 2 in Fig. 7 degenerate into solutions of the first family on the lower part of curve 2 in Fig. 7. Thus, for Ka = 2, nonuniqueness of families of steady traveling solutions exists only in a small range of wavenumbers. The absence of oscillations on the leading front of the long waves of solutions obtained by continuation from the wave of the first family with increasing Re (beginning from Re = 0.2) and for $\lambda_{\text{neut}}/\lambda = \text{const}$, Ka = 2 should be noted (Fig. 9).

The results obtained allow us to draw the following conclusions. The Navier–Stokes calculations of nonlinear wavy regimes and their stability have some differences from the calculations by the integral model. Branching of new families of steady traveling solutions is possible only with doubling of their period. As a consequence, there are only several families of steady traveling solutions. Calculations by the integral model yield a countable number of different families of such solutions.

For high Reynolds numbers, the solutions found imply the existence of an internal vortex zone moving with the phase velocity of the wave.

This work was supported by the Russian Foundation for Basic Research (Grant No. 08-08-00421).

REFERENCES

1. W. Nusselt, "Die Oberflächenkondensation des Wasserdampfes," *Z. VDI*, **60**, 541–546 (1916).
2. P. L. Kapitsa, "Wavy flow of thin layers of a viscous liquid," *Zh. Éksper. Teor. Fiz.*, **18**, No. 1, 3–28 (1948).
3. T. B. Benjamin, "Wave formation in laminar flow down on inclined plane," *J. Fluid Mech.*, **2**, 554–574 (1957).
4. C. S. Yih, "Stability of liquid flow down an inclined plane," *Phys. Fluids*, **6**, 321–334 (1963).
5. A. A. Nepomnyashchii, "Stability of wavy regimes in a film flowing down an inclined plane," *Izv. Akad. Nauk SSSR, Mekh. Zhidk. Gaza*, No. 3, 28–33 (1974).
6. O. Yu. Tsvelodub, "Solitons in a down-flowing film with moderate mass flow rates of the liquid," *J. Appl. Mech. Tech. Phys.*, **21**, No. 3, 345–346 (1980).
7. H.-C. Chang, "Wave evolution on a falling film," *Annu. Rev. Fluid Mech.*, **26**, 103–136 (1994).
8. L. T. Nguyen and V. Balakotaiah, "Modeling and experimental studies of wave evolution on free falling viscous films," *Phys. Fluids*, **12**, 2236–2256 (2000).
9. H.-C. Chang and E. A. Demekhin, *Complex Wave Dynamics on Thin Films*, Elsevier, New York (2002).
10. S. V. Alekseenko, V. E. Nakoryakov, and B. G. Pokusaev, *Wavy Liquid Film Flow* [in Russian], Nauka, Novosibirsk (1992).
11. M. Vlachogiannis and V. Bontozoglou, "Observations of solitary wave dynamics of film flows," *J. Fluid Mech.*, **435**, 191–215 (2001).
12. V. Ya. Shkadov, "Wavy modes of gravity-driven viscous thin-film flow," *Izv. Akad. Nauk SSSR, Mekh. Zhidk. Gaza*, No. 1, 43–51 (1967).

13. E. A. Demekhin and V. Ya. Shkadov, "Regimes of two-dimensional waves in a thin layer of a viscous liquid," *Izv. Akad. Nauk SSSR, Mekh. Zhidk. Gaza*, No. 3, 63–67 (1985).
14. Yu. Ya. Trifonov and O. Yu. Tsvelodub, "Nonlinear waves on the surface of a falling liquid film. 1. Waves of the first family and their stability," *J. Fluid Mech.*, **229**, 531–554 (1991).
15. R. W. Chin, F. H. Abernathy, and J. R. Bertschy, "Gravity and shear wave stability of free surface flows. 1. Numerical calculations," *J. Fluid Mech.*, **168**, 501–513 (1986).
16. T. R. Salamon, R. C. Armstrong, and R. A. Brown, "Traveling waves on inclined films: numerical analysis by the finite-element method," *Phys. Fluids*, **6**, 2202–2220 (1994).
17. P. Bach and J. Villadsen, "Simulation of the vertical flow of a thin wavy film using a finite element method," *Int. J. Heat Mass Transfer*, **2**, 815–827 (1984).
18. Yu. Ya. Trifonov, "Viscous liquid film flows over a periodic surface," *Int. J. Multiphase Flow*, **24**, 1139–1161 (1998).